AIP | Journal of Applied Physics

External electric field induced oxygen-driven unzipping of carbon nanotubes

Hongpeng Zhao, Wei Xu, Liang Song, Qinggao Mei, Chi Chen et al.

Citation: J. Appl. Phys. **112**, 074316 (2012); doi: 10.1063/1.4757587
View online: http://dx.doi.org/10.1063/1.4757587
View Table of Contents: http://jap.aip.org/resource/1/JAPIAU/v112/i7
Published by the American Institute of Physics.

External electric field induced oxygen-driven unzipping of carbon nanotubes

Hongpeng Zhao, Wei Xu, Liang Song, Qinggao Mei, Chi Chen, Ling Miao,[a)] and Jianjun Jiang

Department of Electronic Science and Technology, Huazhong University of Science and Technology, Wuhan, Hubei 430074, People's Republic of China

(Received 10 July 2012; accepted 5 September 2012; published online 8 October 2012)

Based on density functional theory, the mechanisms for oxygen-driven unzipping of carbon nanotubes under electric field are presented. Under the control of external electric field, O adatoms will diffuse along the single-walled carbon nanotube from low potential to the high potential sites. The energy barrier of O adatoms diffusion gets lower while increasing the electric potential, thus enabling the O adatoms to diffuse to the higher potential sites more easily. And with quantities of O adatoms diffusing to the high potential sites, a linear epoxy chain is formed and the single-walled carbon nanotube will be unzipped into graphene nanoribbons automatically. © *2012 American Institute of Physics*. [http://dx.doi.org/10.1063/1.4757587]

I. INTRODUCTION

Graphene nanoribbons (GNRs) are one-dimensional strip of single carbon layer with a width in nanometer scale. It is a potential candidate for nanoelectronics, spintronics, and nanoelectromechanical systems because of its distinctive edge states and electronic properties.[1–4] So far, lots of methods have been tested to fabricate GNRs.[5] Strong oxidants, such as $KMnO_4$, H_2SO_4, and HNO_3 can open carbon nanotubes longitudinally,[6,7] but graphene nanoribbons made in this way would be easily over oxidized, while this can be improved by applying electrochemistry method and annealing procedure.[8] The technique of current-induced electrical break-down of multi-walled carbon nanotubes (MWCNTs) to produce GNRs[9] and applying high dc pulse are also alternatives.[10] Moreover, metal nanoparticles (Ni or Co),[11] splitting using potassium vapor,[12] and plasma etching[13] offer efficient ways to obtain qualified GNRs. When molecules such as hydrogen, oxygen, and ammonia are absorbed on the surface of nano-materials, the electronic properties of the nano-materials will be changed largely.[14–16] The extensive literature has proved oxidation to be optional in unzipping nano-materials.[17,18] Sun and Fabris have studied the energetics for the formation and growth of an extended linear defect from the O diffusion to the ether trimer in graphene.[19] Silva-Tapia *et al.* elaborated the oxygen migration process, which highlights the origin of epoxide groups.[20]

Many scholars have argued that the electric field reforms the electronic properties such as Fermi level, band gaps, carrier transport of the nano-materials, thus inducing the bonding energy, adsorption, and diffusion processes to be changed in accordance.[21–26] The applied electric field has rendered nano-materials with super abilities to store hydrogen, absorp oxygen, detect SO_2 gas, and so on.[27–31]

In this paper, we verify the control of electric field which enables the absorbed O adatoms to form a linear epoxy alignment, and then unzip a single-walled carbon nanotube (SWCNT) after oxidation. And the strength of the electric field is changed to analyze the variation of energy barrier of O adatom's diffusion.

II. COMPUTATIONAL METHODOLOGY

Our calculations are carried out by the density-functional theory (DFT)[32,33] implemented in SIESTA code.[34] The local density approximation (LDA)[33] and Ceperley-Alders exchange-correlation potential parametrized by Perdew-Zunger scheme (CA-PZ)[35] are used. The ***k***-point is set to $1 \times 1 \times n$ Monkhorst-Pack mesh. The cut-off energy is 120 Ry. All structures are optimized until the force on each atom is less than 0.05 eV/Å. The self-consistent electronic iterations are run until energy change falls below 10^{-4} eV.

We consider 5 unit cells of a SWCNT (3,3) in a supercell of size 18 Å × 18 Å × 12.298 Å with the tube axis taken along z-direction. Therefore, a vacuum space of approximate 10 Å is introduced between the neighboring tubes. On the surface of the SWCNT, the O adatoms are absorbed on two epoxy equilibrium states (Figure 1, site A and site B) and a transition state (TS) (Figure 1, site T) which has a single C–O bond, and the transition state is chosen as the energy barrier for it holds higher energy along the reaction pathway of O adatom diffusion around the SWCNT.[22] Moreover, the direction of external electric field is perpendicular to the axis of the SWCNT.

III. RESULTS AND DISCUSSION

A. O adatom's diffusion under electric field

External electric field has very big effect on the properties of the three states (Figure 1, site A, B, and T). The energy of equilibrium states (site A and B) and transition state (site T) is shown in Figure 2. Calculation results show that transition state (site T) holds higher energy than equilibrium states (site A and B). Without the effect of electric field, the C–C bond underneath the absorbed oxygen adatom at the epoxy equilibrium state (Figure 2, site A) is stretched to 2.078 Å, while the one underneath the absorbed oxygen

[a)]Electronic mail: miaoling@mail.hust.edu.cn.

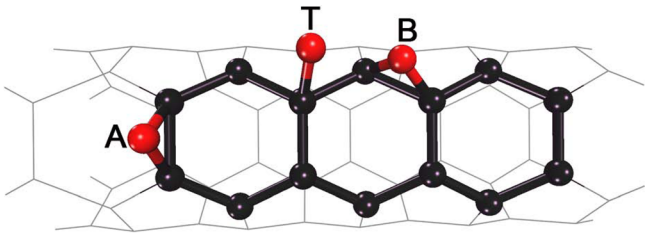

FIG. 1. O adatoms at different sites of the SWCNT. Site A and site B for the equilibrium states with epoxide and site T for the transition state with a single C–O bond. The black and red balls are carbon and oxygen atoms, respectively.

adatom (Figure 2, site T) is stretched to 1.482 Å. The C–C bonds below the O adatom are broken during the structural optimization, demonstrating that the state (Figure 2, site A) with lower energy is more stable. However, under the effect of electric field the difference between the energy of equilibrium states and transition states decreases by certain value, which proves that electric field makes it easier for the O adatom to diffuse from site A to site B much easier. And a similar result was reported in a recent study by Suarez.[22]

Under electric field of 1 V/Å, the energy of the equilibrium states decreases from A1 to A4 while increasing the potential, and the states from B1 to B3 hold the similar tendency, as shown in Figure 3. Therefore, O atom is inclined to absorb on the high potential sites (site A or B) of SWCNT. Moreover, it is interesting to find out that the energy barrier from site A1 to site B1 (A2 to B2 and A3 to B3, likely) gets lower along the direction of high electric potential, and the energy barrier from site B1 to site A2 (B2 to A3 and B3 to A4, likely) gets lower at the same time. Thus with the effect of electric field and lattice thermal vibration, the O adatom can diffuse along the SWCNT to the high potential site more easily. The results also show that the energy barrier of O adatom diffusion around high potential from B3 to A4 is only 0.16 eV, which is largely lower than the energy barrier at low potential site from A1 to B1. As it is important to find method to fabricate GNRs with smooth edges, in the following analysis we focus on calculate the energy barrier of O

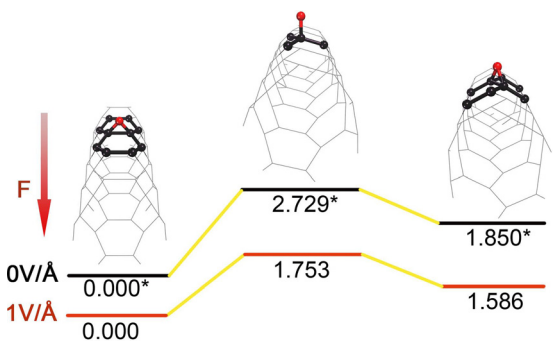

FIG. 2. Site A and B for the equilibrium states, and site T for the transition states with a single C–O bond. The data for configurations without the effect of electric field are marked by a "*". The O adatoms are all absorbed at the highest potential sites of the SWCNT and the direction of electric field (1 V/Å) is perpendicular to the axis of SWCNT, indicated by the arrow. The black and red balls are carbon and oxygen atoms, respectively. All energies are in eV.

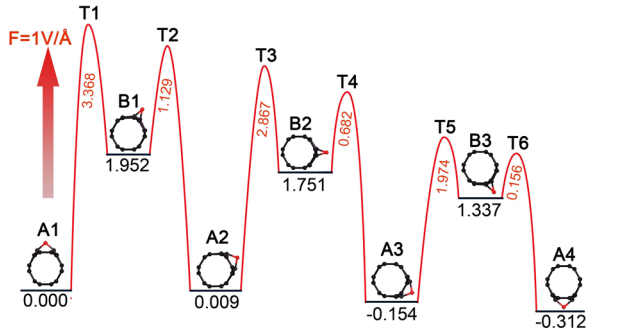

FIG. 3. The energy barriers of oxygen adatom diffusion from low potential to high potential. A1–A4 and B1–B3 for the equilibrium states. T1–T6 for the transition states. The direction of the electric field of 1 V/Å is indicated by the arrow. The black and red balls are carbon and oxygen atoms, respectively. All energies are in eV.

adatom diffusion around the high potential sites under electric field.

Figure 4 displays the geometric parameters around the O adatom of equilibrium state and transition state when it diffuses from low potential to high potential. After a detailed observation we note that the C-C distances underneath the absorbed oxygen adatom in configurations (Figure 4, A1–A4) become longer and longer, so are the C–O bonds in configurations (Figure 4, A1–A4), which indicates that the total energy in configurations (Figure 4, A1–A4) appears to be in a downward trend. The similar analysis still holds true to the total energy of configurations (Figure 4, B1–B3). As for the transition states (T1–T6), along the direction of high electric potential, the C–O bond distance as well as the angle CCO of configurations (Figure 4, T1, T3, T5) becomes larger and the total energy of the system gets lower simultaneously. The configurations (Figure 4, T2, T4, T6) have the similar tendency.

B. O adatom's diffusion under different electric fields

We now turn to figure out the diffusion of O adatom while changing the strength of electric field from 0 V/Å to 3 V/Å, as schematically shown in Figure 5. Without the electric field, the O adatom at initial state (IS) needs 0.88 eV to turn to TS, but the energy barrier can be decreased to 0.16 eV while applying an electric field of 1 V/Å. In addition, if the strength of electric field increases to 2 V/Å, the energy barrier gets down to −0.88 eV. And it is interesting to find that the energy barrier is negative, implying that the O adatom can diffuse from IS to final state (FS) automatically. But a too strong electric field (3 V/Å in this study) will cause an apparent distortion of the SWCNT, and make the transition state of Figure 5 (TS) maintains the lowest energy. In summary, stronger electric field within a reasonable range can be applied to improve the activity and fluxion of the O adatom.

Figure 5 also shows the geometric parameters around the O adatom of IS, TS, and FS. From the FS, we get to understand why the C–C bonds length underneath the oxygen adatom stretches with the increase of the electric field strength, which breaks up the C–C bonds and makes a more stable structure system, and the C–O bonds of the terminal states get longer at the same time. We could also judge

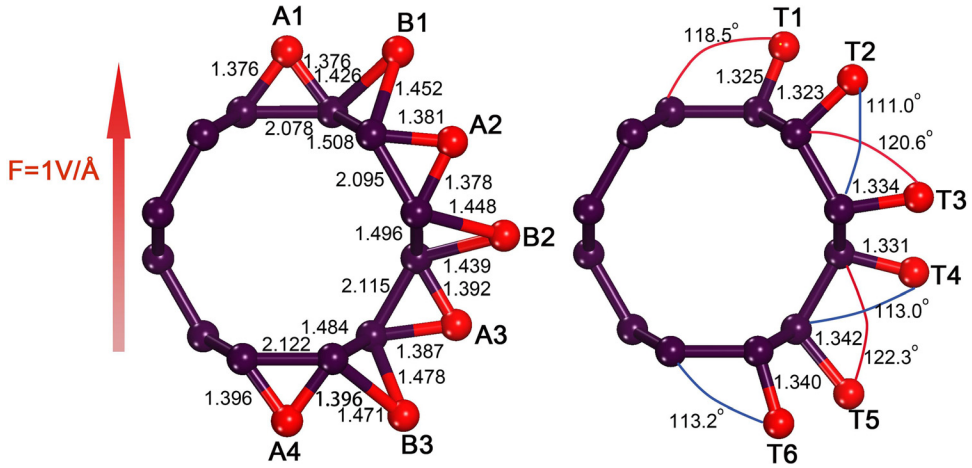

FIG. 4. The geometric parameters (bond length in Å, bond angle in o) around O adatom of equilibrium states (left hand) and transition states (right hand) when it diffuses from low potential to high potential. The states of (site A, B, and T) match with Figure 3 (site A, B, and T). The direction of the electric field is indicated by the arrow. The black and red balls are carbon and oxygen atoms, respectively.

from the TS that the C–O bonds length increases with stronger electric field, since the negative oxygen ion in the system suffers bigger acting force under stronger electric field, the C–O bonds length gets larger. Moreover, the energy barrier gets lower and even turns to be negative, as reported Figure 5.

C. Unzipping of carbon nanotubes under external electric field

In this work, our goal is to figure out whether oxygen adatoms can unzip the nanotubes with the help of electric field. So for further study, we now turn to how several O atoms diffuse and analyze the mechanisms for oxidative unzipping of SWCNT under the electric field. At the beginning, we consider two O adatoms on the surface of SWCNT under electric field of 1 V/Å. To simplify the case, we put one O adatom at the high potential site and try to observe the diffusion of the other O adatom at the neighbouring sites, shown as Figure 6 (IS1, IS2, and FS1). Similarly, when we study the structure containing three O adatoms, two O adatoms are put at the high potential site and the third one is moved, shown as Figure 6 (IS3, IS4, and FS2). Besides, we cannot bind two epoxy adatoms above the same C–C bond.

Figure 6 (IS1, IS2, and FS1) shows that the configuration (Figure 6, IS2) releases 1.68 eV and requires an activation energy of 0.12 eV to form the configuration of Figure 6 (FS1). However, the configuration (Figure 6, IS1) can transform to another configuration (Figure 6, FS1) automatically. As the C–C bonds underneath the O adatom are broken in Figure 6 (FS1), the liner epoxy structures are more stable. And the energy barrier is 0.77 eV less than that of oxygen adatom bounce from the same place without electric field in Figure 5. Then, we increase the number of the absorbed O adatoms and analyze the configuration of Figure 6 (IS3, IS4, and FS2). It is verified that the configuration (Figure, 6 IS4) releases 1.54 eV and requires an activation energy of 0.18 eV to turn to the energy-optimized structure (Figure 6, FS2). It

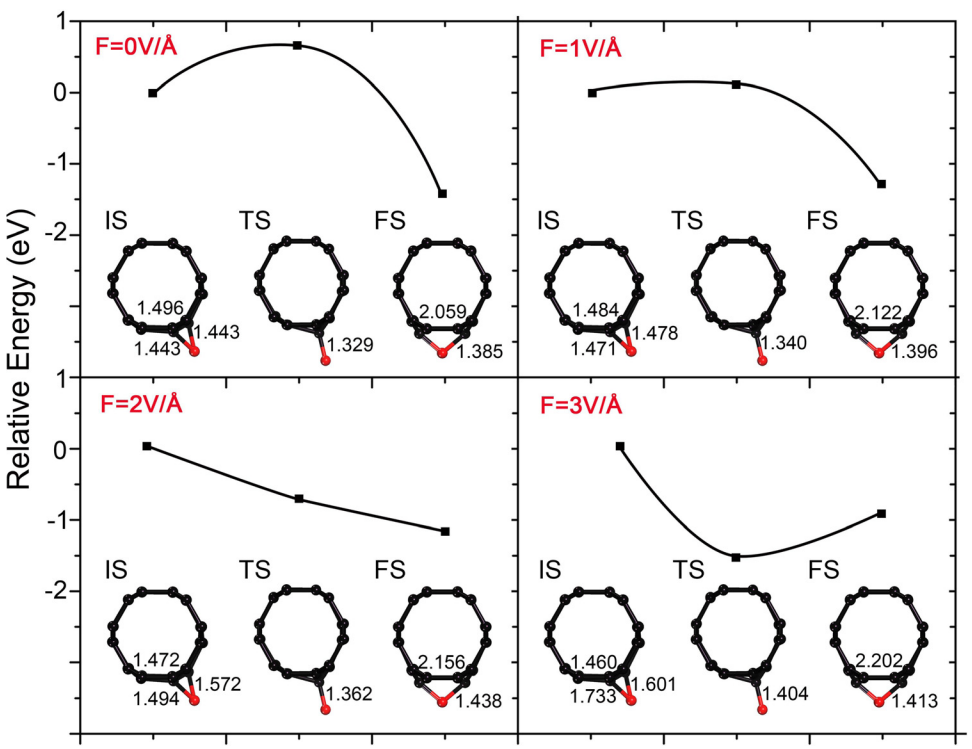

FIG. 5. The energy barriers from initial state of configuration to terminal state of configuration when the strength of electric field changes from 0 V/Å to 3 V/Å. IS, TS, and FS represent initial state, transition state, and final state, respectively. The energy of IS is taken to be zero. The black and red balls are carbon and oxygen atoms, respectively. All energies are in eV.

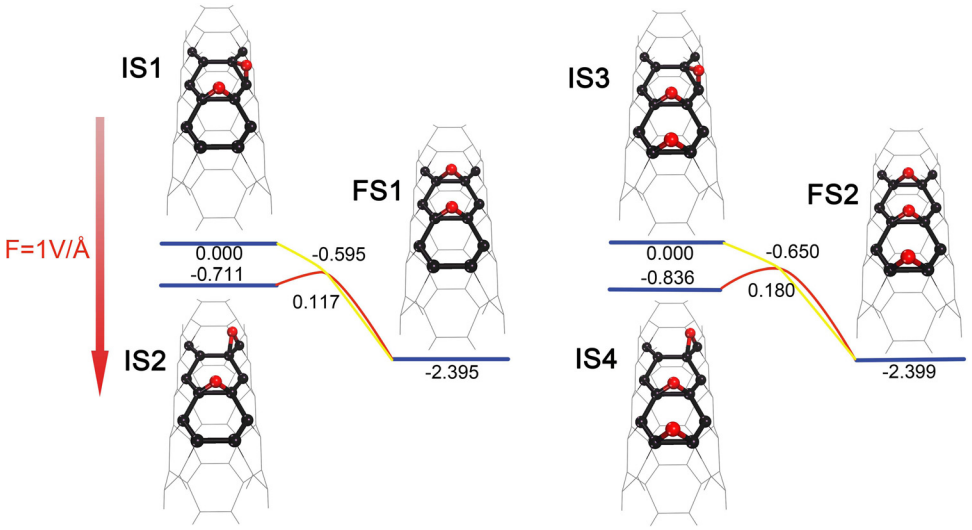

FIG. 6. The configurations (IS1, IS2, and FS1) are for the energy barrier of the second oxygen adatom diffuses to the highest potential. The configurations (IS3, IS4, and FS2) are for the energy barrier of the third oxygen adatom diffuses to the highest potential. The direction of the electric field is indicated by the arrow. The black and red balls are carbon and oxygen atoms, respectively. All energies are in eV.

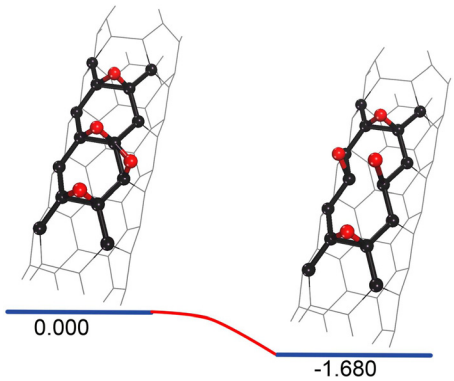

FIG. 7. The energy barrier of the fourth oxygen adatom diffuses to the highest potential. The epoxy structure turns into two semi-quinones automatically (FS). All energies are in eV. The black and red balls are carbon and oxygen atoms, respectively.

is interesting to find out that the C–C bonds length below the oxygen adatom in Figure 6 (FS2) becomes longer than that of Figure 6 (FS1) by 0.014 Å. So with the increase of linear epoxy adatoms, the C–C bonds length underneath the oxygen adatoms gets longer. And the overlap population between the C–C bonds changes from −0.005 in Figure 6 (FS1) to −0.004 in Figure 6 (FS2), which certifies that both C–C bonds underneath the O adatom have been broken.

Then, we consider the condition of one O adatom in presence of more linear O adatoms displayed in Figure 7 (IS). The epoxy structure can turn into two semi-quinones automatically shown in Figure 7 (FS), which is 0.17 eV lower. The C–C bonds length is about 2.906 Å, the calculated overlap population for the C–C bonds is only 0.007, which proves that the C–C bonds are totally broken up. When large quantities of the C–O–C bonds are broken along the linear epoxy adatoms, a nanoribbon could be formed by unzipping and cutting of SWCNT.

IV. CONCLUSION

In conclusion, The diffusion of O adatoms on SWCNT (3,3) and possibility to unzip the SWCNT under external electric field are investigated using DFT calculation. The energy barrier of O adatom diffusion turns lower with the increase of the potential. With the electric field verifies from 0 V/Å to 2 V/Å, the energy barrier of O adatom diffusion gets lower around the high potential. Having large quantities of O adatoms diffusing to form a linear epoxy structure, the SWCNT is cut and unzipped to form GNRs. Our study not only finds another key to produce GNRs but also promotes oxidation to be carried out experimentally. Moreover, in this work we propose a promising approach to fabricate various nano-devicies based on SWCNT.

[1]K. Novoselov, Nature Mater. **6**, 720 (2007).
[2]O. Hod, V. Barone, J. E. Peralta, and G. E. Scuseria, Nano Lett. **7**, 2295 (2007).
[3]L. Yang, C. H. Park, Y. W. Son, M. L. Cohen, and S. G. Louie, Phys. Rev. Lett. **99**, 186801 (2007).
[4]M. Y. Han, B. Ozyilmaz, Y. Zhang, and P. Kim, Phys. Rev. Lett. **98**, 206805 (2007).
[5]X. Jia, J. C. Delgado, M. Terrones, V. Meunier, and M. S. Dresselhaus, Nanoscale **3**, 86 (2011).
[6]N. L. Rangel, J. C. Sotelo, and J. M. Seminario, J. Chem. Phys. **131**, 031105 (2009).
[7]V. Kosynkin, A. L. Higginbotham, A. Sinitskii, J. R. Lomeda, A. Dimiev, B. K. Price, and J. M. Tour, Nature **458**, 872 (2009).
[8]B. Shinde, J. Debgupta, A. Kushwaha, M. Aslam, and V. K. Pillai, J. Am. Chem. Soc. **133**, 4168 (2011).
[9]K. Kim, A. Sussman, and A. Zettl, ACS Nano **4**, 1362 (2010).
[10]W. S. Kim, S. Y. Moon, S. Y. Bang, B. G. Choi, H. Ham, T. Sekino, and K. B. Shim, Appl. Phys. Lett. **95**, 083103 (2009).
[11]A. L. Elías, A. R. Botello-Méndez, D. Meneses-Rodríguez, V. J. Gonźlez, D. Ramírez-Gonźlez, L. Ci, E. Muñoz-Sandoval, P. M. Ajayan, H. Terrones, and M. Terrones, Nano Lett. **10**, 366 (2010).
[12]D. V. Kosynkin, W. Lu, A. Sinitskii, G. Pera, Z. Sun, and J. M. Tour, ACS Nano **5**, 968 (2011).
[13]L. Y. Jiao, L. Zhang, X. R. Wang, G. Diankov, and H. J. Dai, Nature **458**, 877 (2009).
[14]F. Schedin, A. K. Geim, S. V. Morozov, E. W. Hill, P. Blake, M. I. Katsnelson, and K. S. Novoselov, Nature Mater. **6**, 652 (2007).
[15]E. Romero, P. Joshi, A. K. Gupta, H. R. Gutierrez, M. W. Cole, S. A. Tadigadapa, and P. C. Eklund, Nanotechnology **20**, 245501 (2009).
[16]S. Ryu, L. Liu, S. Berciaud, Y. Yu, H. Liu, P. Kim, G. W. Flynn, and L. E. Brus, Nano Lett. **10**, 4944 (2010).
[17]J. L. Li, K. N. Kudin, M. J. McAllister, R. K. Prud'homme, I. A. Aksay, and R. Car, Phys. Rev. Lett. **96**, 176101 (2006).
[18]F. Li, E. Kan, R. Lu, C. Xiao, K. Deng, and H. Su, Nanoscale **4**, 1254 (2012).

[19]T. Sun and S. Fabris, Nano Lett. **12**, 17 (2012).
[20]A. B. Silva-Tapia, X. Garcia-Carmona, and L. R. Radovic, Carbon **50**, 1152 (2012).
[21]K. S. Novoselov, A. K. Geim, S. V. Morozov, D. Jiang, Y. Zhang, S. V. Dubonos, I. V. Grigorieva, and A. A. Firsov, Science **306**, 666 (2004).
[22]A. M. Suarez, L. R. Radovic, E. Bar-Ziv, and J. O. Sofo, Phys. Rev. Lett. **106**, 146802 (2011).
[23]V. J. Surya, K. Iyakutti, H. Mizuseki, and Y. Kawazoe, Int. J. Hydrogen Energy **36**, 13645 (2011).
[24]Y. Lu, L. Shi, C. Zhang, and Y. Feng, Phys. Rev. B **80**, 233410 (2009).
[25]A. K. Geim, Science **324**, 1530 (2009).
[26]K. Geim and K. S. Novoselov, Nature Mater. **6**, 183 (2007).
[27]W. Liu, Y. H. Zhao, J. Nguyen, Y. Li, Q. Jiang, and E. J. Lavernia, Carbon **47**, 3452 (2009).
[28]Y. Sato, K. Takai, and T. Enoki, Nano Lett. **11**, 3468 (2011).
[29]J. Zhou, Q. Wang, Q. Suna, P. Jena, and X. S. Chenb, Proc. Natl. Acad. Sci. U.S.A. **107**, 2801 (2010).
[30]Y. B. Jia, G. L. Zhuang, and J. G. Wang, J. Phys. D: Appl. Phys. **45**, 065305 (2012).
[31]Z. M. Ao and F. M. Peeters, J. Phys. Chem. C **114**, 14503 (2010).
[32]P. Hohenberg and W. Kohn, Phys. Rev. **136**, B864 (1964).
[33]W. Kohn and L. J. Sham, Phy. Rev. **140**, A1133 (1965).
[34]J. M. Soler, E. Artacho, J. D. Gale, A. Garcia, J. Junquera, P. Ordejon, and D. S. Portal, J. Phys.: Condens. Matter **14**, 2745 (2002).
[35]J. P. Perdew and A. Zunger, Phys. Rev. B **23**, 5048 (1981).